Available online at www.sciencedirect.com
ScienceDirect
International Journal of Heat and Fluid Flow 28 (2007) 777–786
International Journal of HEAT AND FLUID FLOW
www.elsevier.com/locate/ijhff

Prediction of temperature distribution and Nusselt number in rectangular microchannels at wall slip condition for all versions of constant heat flux

Lütfullah Kuddusi *, Edvin Çetegen

Istanbul Technical University, Faculty of Mechanical Engineering, Mechanical Engineering Department, Gümüşsuyu, 34437 Istanbul, Turkey

Received 11 February 2005; received in revised form 12 September 2006; accepted 13 September 2006
Available online 7 November 2006

Abstract

Slip-flow in rectangular microchannels heated at constant and uniform heat flux (H2 boundary condition) is studied. The study is extended to the eight possible thermal versions that are formed of different combinations of heated and adiabatic walls. The paper aims to show the effect of different thermal versions on heat transfer in microchannel. The velocity distribution that is required in determining of temperature distribution is obtained from the literature. Mathematical similarity between the heat conduction and convection problems is used to determine the temperature distribution in the microchannel. The solution of a heat conduction problem, available in the literature, is adapted to the heat convection problem in the microchannel. The velocity and temperature distributions thus found are used to determine the average Nusselt number for all the eight thermal versions. For the case studied, it is found that rarefaction has a decreasing effect on heat transfer in the microchannels exposed to any of the eight thermal versions. The results of the paper for the special case of no-slip-flow agree exactly with the results found for macrochannels in the literature.

Keywords: Microchannel; Slip-flow; Convective heat transfer; Nusselt number; Knudsen number

1. Introduction

Slip-flow occurs if the flow pressure is very low or the characteristic size of the flow system is small. Continuum physics is no longer valid if the characteristic size of the flow system is comparable to the molecular mean free path. In no-slip-flow, as a requirement of continuum physics, the flow velocity is zero at a fluid–solid interface and the fluid temperature immediately adjacent to the solid walls is equal to that of the solid walls. In the presence of slip-flow, the flow velocity at the solid walls is nonzero and there is a temperature jump (a finite difference between the temperatures of solid wall and the adjacent fluid). These nonzero flow velocity and temperature jump at the solid walls are major hydrodynamic and thermal effects that need to be taken into account in slip-flow solutions.

Slip-flow solutions in microchannels may be investigated for two cases; when the walls of the microchannel are heated at constant and uniform temperature (H1 boundary condition) and; when the walls of the microchannel are heated at constant and uniform heat flux (H2 boundary condition). In the literature, each of these cases may be divided into eight sub-versions that are formed from different combinations of heated and adiabatic walls. Morini (2000) and Spiga and Morini (1996) have solved the flow in macrochannels for all the eight thermal versions of the H1 and H2 boundary conditions, respectively. Tunc and Bayazitoglu (2002) have solved the slip-flow in microchannels exposed to H2 boundary condition for the specific case when all the walls of microchannel are heated at constant and uniform heat flux. They determined the Nusselt

* Corresponding author. Tel.: +90 212 2931300x2452; fax: +90 212 2450795.
E-mail addresses: kuddusi@itu.edu.tr (L. Kuddusi), cetegenedv@itu.edu.tr (E. Çetegen).

0142-727X/$ - see front matter © 2006 Elsevier Inc. All rights reserved.
doi:10.1016/j.ijheatfluidflow.2006.09.002

Nomenclature

a	long side of microchannel
A	constant defined by Eq. (52)
b	short side of microchannel
b_1, b_2, b_3	constants defined by Eqs. (15)–(17)
c_P	specific heat
d_1, d_2, d_3, d_4	constants equal to 1 or 0
D_h	hydraulic diameter
g	heat generation function
$\bar{g}$	transformed heat generation function defined by Eq. (53)
h	convection heat transfer coefficient
k	thermal conductivity
K	kernel
Kn	Knudsen number
L_h	heated perimeter of microchannel
Nu	Nusselt number
p	fluid pressure
P	normalized pressure gradient
Pr	Prandtl number
q	heat flux
R	specific heat ratio
S_1, S_2, S_3, S_4	constants introduced for simplicity defined by Eqs. (25)–(28)
T	temperature
$\widehat{T}$	nondimensional temperature
u	fluid velocity
$\widehat{u}$	nondimensional fluid velocity
x, y, z	nondimensional coordinates

Greek symbols

α	thermal diffusivity
β_m	eigenvalues for the energy equation
β_t	dimensionless variable defined by Eq. (3)
β_v	dimensionless variable defined by Eq. (4)
γ	aspect ratio (b/a)
λ_{mfp}	molecular mean free path
μ	dynamic viscosity
μ_n	eigenvalues for the momentum equation
ν_n	eigenvalues for the energy equation
ρ	density
ξ, η, ζ	coordinates

Subscripts

b	bulk property
j	index
m	mean value
m	index
n	index
s	fluid property near the wall
w	wall value
0	inlet property

number for various rarefaction intensities and microchannel aspect ratios, and found that rarefaction has a decreasing effect on the heat transfer. Ghodoossi and Egrican (2005) solved the slip-flow in microchannels exposed to H1 boundary condition for the specific case when all the walls of the microchannel are heated at constant and uniform temperature. Similar heat transfer behaviors are reported as those in the work of Tunc and Bayazitoglu (2002).

In this paper, the slip-flow in microchannels exposed to H2 boundary condition is studied for all the eight thermal versions. The paper aims to show the effect of different thermal boundary conditions on heat transfer in microchannel. Temperature distribution and Nusselt number are determined. The results for the special case of zero rarefaction (solution for macrochannel) agree exactly with the results of Spiga and Morini (1996) who solved the macrochannel flow for the same eight thermal versions. Part of the results for slip-flow regime, which is the main concern of the paper, is in agreement with that of Tunc and Bayazitoglu (2002) and Yu and Ameel (2002).

2. Problem statement

The problem under consideration is a hydrodynamically and thermally developed steady flow in the rectangular microchannel shown in Fig. 1. It is supposed that the dimensions of the microchannel are comparable to the molecular mean free path. According to the explanations above, a slip-flow will occur in the microchannel. That is, a nonzero flow velocity and a temperature jump will occur at the walls of the microchannel. The properties of such a slip-flow are quantified by the Knudsen number Kn, which is defined as the ratio of the molecular mean free path to the characteristic length of microchannel. According to Beskok and Karniadakis (1992), no-slip-flow (flow in macrochannels) occurs if the Knudsen number is lower than 0.001 and, the slip-flow (flow in microchannels) occurs if the Knudsen number ranges from 0.001 to 0.1, which is

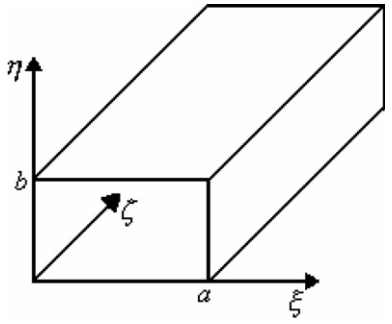

Fig. 1. The geometry of microchannel.

the range of interest considered in this paper. That is, the characteristic size of microchannels considered in the paper is less than 100 μm if air with mean free path equal to 0.066 μm (at standard conditions) is the flowing fluid.

If the problem under consideration was a no-slip-flow, the temperature of the flow near the wall, T_s, would be equal to the wall temperature, T_w, and the velocity of the flow near the wall, u_s, would be equal to zero. Since the problem under consideration is a slip-flow, the temperature of the flow near the wall is no longer equal to the wall temperature and the velocity of the flow near the wall is no longer zero. The temperature and velocity of the flow at the bottom wall, first-order slip boundary conditions, are given by Barron et al. (1997), as

$$T_s = T_w + \beta_t \lambda_{mfp} \left.\frac{\partial T}{\partial \eta}\right|_{\eta=0} \tag{1}$$

$$u_s = \beta_v \lambda_{mfp} \left.\frac{\partial u}{\partial \eta}\right|_{\eta=0} \tag{2}$$

where the parameters β_v and β_t are given as

$$\beta_t = \frac{2-F_t}{F_t}\frac{2R}{1+R}\frac{1}{Pr} \tag{3}$$

$$\beta_v = \frac{2-F_v}{F_v} \tag{4}$$

The coefficients F_v and F_t are the tangential momentum accommodation coefficient and the thermal accommodation coefficient, respectively. For real walls some molecules reflect diffusively and some reflect specularly. These coefficients are defined as the fraction of molecules reflected diffusively. Depending on the fluid, the solid and the surface finish these coefficients vary from 0 to 1. However, for most engineering applications, values for the accommodation coefficients are near unity. The relations above are used to calculate local temperature jump and slip velocity at solid walls. The local values averaged over the heated perimeter of the microchannel are then used in the Nusselt number calculation. It should be noted that the accuracy of first-order slip boundary conditions begins to deteriorate (Hadjiconstantinou, 2003; Hadjiconstantinou and Simek, 2002) around and beyond $Kn = 0.1$. An appropriate second order slip model (Karniadakis and Beskok, 2002) may improve the accuracy.

The H2 boundary condition can be applied to a rectangular microchannel in eight different versions of heated (at constant heat flux) and adiabatic walls. In the literature (Morini, 2000; Spiga and Morini, 1996), these versions are given as

4 version: Four walls are heated.
3L version: Three walls are heated, one short wall is adiabatic.
3S version: Three walls are heated, one long wall is adiabatic.
2L version: Two walls are heated, two short walls are adiabatic.
2S version: Two walls are heated, two long walls are adiabatic.
2C version: One short and one long wall are heated, the other two walls are adiabatic.
1L version: One long wall is heated, the other three walls are adiabatic.
1S version: One short wall is heated, the other three walls are adiabatic.

The slip-flow in a microchannel with eight different H2 thermal versions above will be solved by applying the Navier–Stokes equations.

3. Momentum equation

The ζ-direction momentum equation for a hydrodynamically developed flow is

$$\frac{\partial^2 u}{\partial \xi^2} + \frac{\partial^2 u}{\partial \eta^2} = \frac{1}{\mu}\frac{\partial p}{\partial \zeta} \tag{5}$$

The modified hydrodynamic boundary conditions according to the slip-flow assumption are

$$u = u_s \quad \text{at } \xi = 0, \quad \xi = a, \quad \eta = 0, \quad \eta = b \tag{6}$$

The momentum equation and the modified boundary conditions are nondimensionalized by introducing the following nondimentional variables

$$x = \frac{\xi}{a}, \quad 0 \leqslant x \leqslant 1 \tag{7}$$

$$y = \frac{\eta}{a}, \quad 0 \leqslant y \leqslant \gamma \equiv \frac{b}{a} \tag{8}$$

$$\widehat{u}(x,y) = \frac{u(\xi,\eta)}{u_m} \tag{9}$$

where u_m represents the mean fluid velocity, which is defined as

$$u_m = \frac{1}{ab}\int_0^b \int_0^a u(\xi,\eta)\cdot \mathrm{d}\xi \cdot \mathrm{d}\eta \tag{10}$$

The nondimensional momentum equation and associated boundary conditions for hydrodynamically developed flow are found as

$$\frac{\partial^2 \widehat{u}}{\partial x^2} + \frac{\partial^2 \widehat{u}}{\partial y^2} = P \tag{11}$$

$$\widehat{u} = \widehat{u}_s \quad \text{at } x = 0, \quad x = 1, \quad y = 0, \quad y = \gamma \tag{12}$$

where the normalized pressure gradient P is defined as

$$P = \frac{a^2}{u_m \mu}\frac{\partial p}{\partial \zeta} \tag{13}$$

The momentum equation in slip-flow is already solved by Tunc and Bayazitoglu (2002). Ghodoossi and Egrican

(2005) have applied a similar procedure to find an explicit relation for velocity distribution as

$$\widehat{u}(x,y) = \frac{\widehat{u}_s}{1+e^{\gamma}}(e^{y}+e^{\gamma-y}) + \sum_{n=1}^{\infty} K(\mu_n,y)(b_1 e^{\mu_n x} + b_2 e^{-\mu_n x} - b_3) \tag{14}$$

where

$$b_1 = \sqrt{\frac{2}{\gamma}}\frac{P[-(-1)^n+1]}{\mu_n^3}\frac{-e^{-\mu_n}+1}{e^{\mu_n}-e^{-\mu_n}} \tag{15}$$

$$b_2 = \sqrt{\frac{2}{\gamma}}\frac{P[-(-1)^n+1]}{\mu_n^3}\frac{e^{\mu_n}-1}{e^{\mu_n}-e^{-\mu_n}} \tag{16}$$

$$b_3 = \sqrt{\frac{2}{\gamma}}\frac{[-(-1)^n+1]}{\mu_n^3}\left(P - \frac{\mu_n^2}{1+\mu_n^2}\widehat{u}_s\right) \tag{17}$$

Kernels and eigenvalues for the boundary conditions of the first kind are:

$$K(\mu_n,y) = \sqrt{\frac{2}{\gamma}}\sin\mu_n y \tag{18}$$

$$\sin\mu_n\gamma = 0, \quad \text{or, } \mu_n = \frac{n\pi}{\gamma} \quad n = 1,2,3,\ldots \tag{19}$$

Using the velocity distribution found above, the nondimensional slip velocity $\widehat{u}_s$ and the normalized pressure gradient P, which are still unknowns, may be determined. Eqs. (2) and (10) may be written in terms of nondimensional variables, respectively, as

$$\widehat{u}_s = \frac{2\gamma}{(1+\gamma)}\beta_v Kn\left.\frac{\partial\,\widehat{u}(x,y)}{\partial y}\right|_{y=0} \tag{20}$$

$$1 = \frac{1}{\gamma}\int_0^{\gamma}\int_0^{1}\widehat{u}(x,y)\cdot dx\cdot dy \tag{21}$$

where the Knudsen number Kn is defined as

$$Kn = \frac{\lambda_{\mathrm{mfp}}}{D_h} \tag{22}$$

Combining Eqs. (14), (20) and (21) and solving simultaneously for the nondimensional slip velocity $\widehat{u}_s$ and the normalized pressure gradient P result in

$$\widehat{u}_s = \frac{S_3}{S_1}\frac{\gamma}{2\left[\frac{1+\gamma}{2\gamma\beta_v Kn} - \frac{1-e^{\gamma}}{1+e^{\gamma}}\left(1+\frac{S_3}{S_1}\right) - \frac{4}{\gamma}S_2\left(\frac{S_4}{S_2}-\frac{S_3}{S_1}\right)\right]} \tag{23}$$

$$P = s\frac{1}{8S_1}\left\{\gamma^2 - \widehat{u}_s\left[\frac{2(e^{\gamma}-1)\gamma}{1+e^{\gamma}} + 8S_2\right]\right\} \tag{24}$$

where

$$S_1 = \sum_{n=1}^{\infty}\frac{2\tanh\mu_{2n-1}/2 - \mu_{2n-1}}{\mu_{2n-1}^5} \tag{25}$$

$$S_2 = \sum_{n=1}^{\infty}\frac{1}{\mu_{2n-1}^2(1+\mu_{2n-1}^2)} \tag{26}$$

$$S_3 = \sum_{n=1}^{\infty}\frac{2\tanh\mu_{2n-1}/2 - \mu_{2n-1}}{\mu_{2n-1}^3} \tag{27}$$

$$S_4 = s\sum_{n=1}^{\infty}\frac{1}{1+\mu_{2n-1}^2} \tag{28}$$

4. Energy equation

The energy equation for a thermally developed flow is

$$\frac{\partial^2 T}{\partial\xi^2} + \frac{\partial^2 T}{\partial\eta^2} = \frac{u(\xi,\eta)}{\alpha}\frac{\partial T}{\partial\zeta} \tag{29}$$

The axial variation of fluid temperature for thermally developed flow is approximated in the following form by providing an energy balance for an arbitrary differential $d\zeta$ segment of the microchannel exposed to any of the eight thermal versions.

$$\frac{\partial T}{\partial\zeta} = \frac{q(d_1 b + d_2 b + d_3 a + d_4 a)}{\rho c_P u_m a b} \tag{30}$$

Note that heat enters the microchannel from the walls that are not adiabatic for each thermal version. The coefficients d_i equal 1 for non-adiabatic walls and 0 for adiabatic walls. Various combinations of these numerical values associated with each of the eight thermal versions are given in Table 1.

The energy equation is nondimensionalized by making use of the nondimensional variables defined by Eqs. (7)–(9) and the nondimentional temperature defined as

$$\widehat{T} = \frac{T - T_0}{(qD_h/k)} \tag{31}$$

The nondimensional energy equation is found as

$$\frac{\partial^2\widehat{T}}{\partial x^2} + \frac{\partial^2\widehat{T}}{\partial y^2} = G\cdot\widehat{u}(x,y) \tag{32}$$

where the values of constant G for the eight thermal versions are given in Table 2.

Table 1
The numerical values of coefficients d_i for the eight thermal versions

Version	d_1	d_2	d_3	d_4
4	1	1	1	1
3L	1	0	1	1
3S	1	1	1	0
2L	0	0	1	1
2S	1	1	0	0
2C	1	0	1	0
1L	0	0	1	0
1S	1	0	0	0

Table 2
The values of constant G for the eight thermal versions

Version	4	3L	3S	2L	2S	2C	1L	1S
G	$\left(\frac{\gamma+1}{\gamma}\right)^2$	$\frac{(1+\gamma)(2+\gamma)}{2\gamma^2}$	$\frac{(1+\gamma)(1+2\gamma)}{2\gamma^2}$	$\frac{1+\gamma}{\gamma^2}$	$\frac{\gamma+1}{\gamma}$	$\frac{1}{2}\left(\frac{1+\gamma}{\gamma}\right)^2$	$\frac{1+\gamma}{2\gamma^2}$	$\frac{1+\gamma}{2\gamma}$

5. Thermal boundary conditions

The walls of the microchannel are either adiabatic or heated at a constant heat flux q. The thermal boundary conditions for the thermal versions may be given in the following form in general:

$$\left[-k\frac{\partial T(\xi,\eta)}{\partial \xi}\right]_{\xi=0} = d_1 \cdot q \tag{33}$$

$$\left[k\frac{\partial T(\xi,\eta)}{\partial \xi}\right]_{\xi=a} = d_2 \cdot q \tag{34}$$

$$\left[-k\frac{\partial T(\xi,\eta)}{\partial \eta}\right]_{\eta=0} = d_3 \cdot q \tag{35}$$

$$\left[k\frac{\partial T(\xi,\eta)}{\partial \eta}\right]_{\eta=b} = d_4 \cdot q \tag{36}$$

Substituting appropriate combinations of the coefficients d_i given in Table 1 in the equations above provides the boundary conditions for the thermal versions.

The general form of the thermal boundary conditions Eqs. (33)–(36) may be nondimensionalized as

$$\left[-\frac{\partial \widehat{T}(x,y)}{\partial x}\right]_{x=0} = d_1 \cdot \frac{1+\gamma}{2\gamma} \tag{37}$$

$$\left[\frac{\partial \widehat{T}(x,y)}{\partial x}\right]_{x=1} = d_2 \cdot \frac{1+\gamma}{2\gamma} \tag{38}$$

$$\left[-\frac{\partial \widehat{T}(x,y)}{\partial y}\right]_{y=0} = d_3 \cdot \frac{1+\gamma}{2\gamma} \tag{39}$$

$$\left[\frac{\partial \widehat{T}(x,y)}{\partial y}\right]_{y=\gamma} = d_4 \cdot \frac{1+\gamma}{2\gamma} \tag{40}$$

6. Solution of the energy equation

The nondimensional energy equation (Eq. (32)) should be solved subject to the boundary conditions given by Eqs. (37)–(40). The nondimensional energy equation is mathematically similar to the governing differential equation for a two dimensional steady state heat conduction problem with variable heat generation in the field. The solution for such a heat conduction problem exists in the literature (Ozisik, 1968). The solution for the heat conduction problem will be adapted to the problem under study. The procedure is explained below.

The governing nondimensional differential equation for a steady state heat conduction in a finite rectangle $(0 \leqslant x \leqslant 1,\ \ 0 \leqslant y \leqslant \gamma)$ with variable heat generation $g(x,y)$ is given as

$$\frac{\partial^2 \widehat{T}}{\partial x^2} + \frac{\partial^2 \widehat{T}}{\partial y^2} + \frac{g(x,y)}{k} = 0 \tag{41}$$

It is supposed that the heat generated in the field is dissipated from the boundary surfaces into the surroundings at a uniform and constant temperature. Therefore, the boundary conditions may be given as

$$\left[-k_1\frac{\partial \widehat{T}(x,y)}{\partial x} + h_1\widehat{T}(x,y)\right]_{x=0} = f_1 \tag{42}$$

$$\left[k_2\frac{\partial \widehat{T}(x,y)}{\partial x} + h_2\widehat{T}(x,y)\right]_{x=1} = f_2 \tag{43}$$

$$\left[-k_3\frac{\partial \widehat{T}(x,y)}{\partial y} + h_3\widehat{T}(x,y)\right]_{y=0} = f_3 \tag{44}$$

$$\left[k_4\frac{\partial \widehat{T}(x,y)}{\partial y} + h_4\widehat{T}(x,y)\right]_{y=\gamma} = f_4 \tag{45}$$

The solution of the heat conduction problem, defined by Eqs. (41)–(45), is given by Ozisik (1968) as

$$\widehat{T}(x,y) = \sum_{m=0}^{\infty}\sum_{n=0}^{\infty}\frac{K(\beta_m,x)K(\nu_n,y)A(\beta_m,\nu_n)}{\beta_m^2+\nu_n^2} \tag{46}$$

where the kernels $K(\beta_m,x)$, $K(\nu_n,y)$ and the eigenvalues β_m, ν_n are given as

$$K(\beta_m,x) = N_m\cos(\beta_m x) \tag{47}$$

$$K(\nu_n,y) = N_n\cos(\nu_n y) \tag{48}$$

$$\sin(\beta 1) = 0, \quad \text{or, } \beta = \frac{m\pi}{1}, \ \ m = 0,1,2,3,\ldots \tag{49}$$

$$\sin(\nu\gamma) = 0, \quad \text{or, } \nu = \frac{n\pi}{\gamma}, \ \ sn = 0,1,2,3,\ldots \tag{50}$$

where

$$N_m = \begin{cases} \sqrt{\frac{2}{1}} & m \neq 0 \\ \sqrt{\frac{1}{1}} & m = 0 \end{cases} \qquad N_n = \begin{cases} \sqrt{\frac{2}{\gamma}} & n \neq 0 \\ \sqrt{\frac{1}{\gamma}} & n = 0 \end{cases} \tag{51}$$

The constant $A(\beta_m, v_n)$ is given as

$$A(\beta_m, v_n) = \frac{\alpha}{k}\bar{g}(\beta_m, v_n) + \alpha\left\{\left.\frac{K(\beta_m,x)}{k_1}\right|_{x=0}\cdot\int_{y=0}^{\gamma} K(v_n,y)\cdot f_1\cdot \mathrm{d}y\right\} + \alpha\left\{\left.\frac{K(\beta_m,x)}{k_2}\right|_{x=1}\cdot\int_{y=0}^{\gamma} K(v_n,y)\cdot f_2\cdot \mathrm{d}y\right\} + \alpha\left\{\left.\frac{K(v_n,y)}{k_3}\right|_{y=0}\cdot\int_{x=0}^{1} K(\beta_m,x)\cdot f_3\cdot \mathrm{d}x\right\} + \alpha\left\{\left.\frac{K(v_n,y)}{k_4}\right|_{y=\gamma}\cdot\int_{x=0}^{1} K(\beta_m,x)\cdot f_4\cdot \mathrm{d}x\right\} \quad (52)$$

where

$$\bar{g}(\beta_m, v_n) = \int_{x=0}^{1}\int_{y=0}^{\gamma} K(\beta_m,x)\cdot K(v_n,y)\cdot g(x,y)\cdot \mathrm{d}x\cdot \mathrm{d}y \quad (53)$$

The governing differential equation (Eq. (41)) and the boundary conditions (Eqs. (42)–(45)) of the heat conduction problem will mathematically be identical to the governing differential equation (Eq. (32)) and the boundary conditions (Eqs. (37)–(40)) of the heat convection problem in the microchannel, respectively, by applying the following adaptations into the heat conduction problem,

$$\alpha = k = k_1 = k_2 = k_3 = k_4 = 1 \quad (54)$$

$$h_1 = h_2 = h_3 = h_4 = 0 \quad (55)$$

$$f_1 = d_1\cdot\frac{1+\gamma}{2\gamma} \quad (56)$$

$$f_2 = d_2\cdot\frac{1+\gamma}{2\gamma} \quad (57)$$

$$f_3 = d_3\cdot\frac{1+\gamma}{2\gamma} \quad (58)$$

$$f_4 = d_4\cdot\frac{1+\gamma}{2\gamma} \quad (59)$$

$$g(x,y) = -G\cdot\widehat{u}(x,y) \quad (60)$$

Therefore, we may consider that the solution for the heat conduction problem given by Eqs. (46)–(53) is also the solution for heat convection problem in the microchannel, provided the adaptations given by Eqs. (54)–(60) are implemented into the solution.

The constant $A(\beta_m, v_n)$ given by Eq. (52) is determined below by implementation of the adaptations above. For different combinations of the indices m and n, formed of zero and nonzero values, the constant $A(\beta_m, v_n)$ is found as

For $m \neq 0$ and $n \neq 0$,

$$A(\beta_m, v_n) = \begin{cases} -8PN_nN_mG\sum\limits_{j=1,\text{even}}^{\infty}\frac{j}{\pi\mu_j^2(j^2-n^2)}\frac{(e^{-\mu_j}+e^{\mu_j}-2)}{(\mu_j^2+\beta_m^2)(e^{\mu_j}-e^{-\mu_j})}, & m,n=\text{even} \\ 0, & m,n=\text{else} \end{cases} \quad (61)$$

For $m = 0$ and $n \neq 0$,

$$A(0, v_n) = \begin{cases} \left[\begin{array}{l} -2N_{m=0}N_nG\frac{e^{\gamma}-1}{e^{\gamma}+1}\frac{\widehat{u}_s}{1+v_n^2} + (d_3+d_4)N_{m=0}N_n\frac{1+\gamma}{2\gamma} \\ -2\sqrt{2\gamma}N_{m=0}N_nG\sum\limits_{j=1,\text{even}}^{\infty}\frac{j}{\pi(j^2-n^2)} \\ \times\left(b_{1,j}\frac{e^{\mu_j}-1}{\mu_j} - b_{2,j}\frac{e^{-\mu_j}-1}{\mu_j} - b_{3,j}\right), \end{array}\right. & n=\text{even} \\ \left[(d_3-d_4)N_{m=0}N_n\frac{1+\gamma}{2\gamma}, \right. & n=\text{odd}. \end{cases} \quad (62)$$

For $m \neq 0$ and $n = 0$,

$$A(\beta_m, 0) = \begin{cases} -8PN_{n=0}N_mG\sum\limits_{j=1,\text{even}}^{\infty}\frac{1}{\pi j\mu_j^2}\frac{(e^{-\mu_j}+e^{\mu_j}-2)}{(\mu_j^2+\beta_m^2)(e^{\mu_j}-e^{-\mu_j})} \\ \quad +(d_1+d_2)N_mN_{n=0}\frac{1+\gamma}{2}, & m=\text{even} \\ (d_1-d_2)N_mN_{n=0}\frac{1+\gamma}{2}, & m=\text{odd} \end{cases} \quad (63)$$

For $m = 0$ and $n = 0$ a special case occurs and the constant $A(0,0)$ cannot be evaluated. This is consistent with the H2 type boundary condition that results in a temperature distribution in the form of $\widehat{T}_s(x,y) + C$, where C is a constant. To be able to evaluate the constant C, an additional prescribed condition namely specified temperature on the boundaries or in the flow field is required. The same situation is investigated in the work of Spiga and Morini (1996), who solved the same problem as in this paper but for macrochannels. In the following section of the paper we will show that the value of constant C does not affect the heat transfer (Nusselt number) calculations in the microchannel.

7. Determination of Nusselt number

Integrating the local nondimensional temperature of the fluid at the walls along the heated walls, and averaging over the nondimensional heated perimeter of the microchannel gives the average nondimensional slip temperature $\widehat{T}_s$ as

$$\widehat{T}_s = \frac{d_1\int_0^{\gamma}\widehat{T}(0,y)dy + d_2\int_0^{\gamma}\widehat{T}(1,y)dy + d_3\int_0^{1}\widehat{T}(x,0)dx + d_4\int_0^{1}\widehat{T}(x,\gamma)dx}{d_1\gamma + d_2\gamma + d_3 + d_4} \quad (64)$$

If a no-slip-flow was considered, the nondimensional slip temperature $\widehat{T}_s$ calculated above would be equal to the nondimensional wall temperature $\widehat{T}_w$. Eq. (1) may be nondimensionalized to get,

$$\widehat{T}_w - \widehat{T}_s = -\frac{2\gamma}{1+\gamma}\beta_tKn\left.\frac{\partial\widehat{T}}{\partial y}\right|_{y=0} \quad (65)$$

Since the heat flux imposed on the heated walls is the same (Eqs. (37)–(40)), the nondimensional wall temperature may be calculated on a single heated wall as

$$\widehat{T}_w = \widehat{T}_s + \beta_tKn \quad (66)$$

Determination of the Nusselt number also requires calculation of the bulk or average nondimensional fluid temperature, $\widehat{T}_b$, that is defined as

$$\widehat{T}_b = \frac{1}{\gamma}\int_0^{\gamma}\int_0^{1} \widehat{u}(x,y)\cdot\widehat{T}(x,y)\cdot \mathrm{d}x\cdot \mathrm{d}y \tag{67}$$

Evaluation of the double integrals above leads to

$$\widehat{T}_b = \widehat{T}_{b1} + \widehat{T}_{b2} + \widehat{T}_{b3} + \widehat{T}_{b4} \tag{68}$$

where

$$\widehat{T}_{b1} = 2\widehat{u}_s N_{m=0} N_n \frac{e^{\gamma}-1}{e^{\gamma}+1}\sum_{n=2,\mathrm{odd}}^{\infty}\frac{A(0,v_n)}{v_n^2}\frac{1}{1+v_n^2} \tag{69}$$

$$\widehat{T}_{b2} = \frac{16}{\gamma}N_m N_n P \sum_{j=1,\mathrm{even}}^{\infty}\sum_{m=2,\mathrm{odd}}^{\infty} \times \sum_{n=2,\mathrm{odd}}^{\infty}\frac{A(\beta_m,v_n)(e^{-\mu_j}+e^{\mu_j}-2)}{\mu_j(\mu_j^2+\beta_m^2)(\beta_m^2+v_m^2)(\mu_j^2-v_m^2)(e^{\mu_j}-e^{-\mu_j})} \tag{70}$$

$$\widehat{T}_{b3} = 2\sqrt{\frac{2}{\gamma}}N_{m=0}N_n\sum_{n=2,\mathrm{odd}}^{\infty}\sum_{j=1,\mathrm{even}}^{\infty}\frac{A(0,v_n)}{v_n^2} \times\left(b_{1,j}\frac{e^{\mu_j}-1}{\mu_j} - b_{2,j}\frac{e^{-\mu_j}-1}{\mu_j} - b_{3,j}\right)\frac{\mu_j}{\mu_j^2-v_n^2} \tag{71}$$

$$\widehat{T}_{b4} = \frac{16}{\gamma}N_m N_{n=0} P \sum_{j=1,\mathrm{even}}^{\infty}\sum_{m=2,\mathrm{odd}}^{\infty}\frac{A(\beta_m,0)(e^{-\mu_j}+e^{\mu_j}-2)}{\mu_j^3\beta_m^2(\mu_j^2+\beta_m^2)(e^{\mu_j}-e^{-\mu_j})} \tag{72}$$

With the nondimensional wall and bulk temperatures known, the Nusselt number may now be determined. An energy balance on the heated perimeter at a specified axial cross section of microchannel leads to

$$q\cdot L_h\cdot \mathrm{d}\zeta = h\cdot L_h\cdot \mathrm{d}\zeta\cdot(T_w - T_b) \tag{73}$$

The Nusselt number is calculated by

$$Nu = \frac{h\cdot D_h}{k} \tag{74}$$

By combining Eq. (73) with Eq. (74), and after some manipulation, the Nusselt number is

$$Nu = \frac{1}{\widehat{T}_w - \widehat{T}_b} \tag{75}$$

It can easily be verified that in the calculations above if the temperature $\widehat{T}(x,y)$ is replaced by $\widehat{T}(x,y)+C$ the Nusselt number (Eq. (75)) does not change.

8. Results

All the numerical calculations are carried out using the Mathematica 5 package. Solutions are obtained for $Pr = 0.6$, $R = 1.4$, $F_v = 1$ and $F_t = 1$. A sensitivity analysis on the number of terms in the infinite series indicates that the effect of the terms for n higher than a few hundred disappears. This allows calculating the infinite series with a relatively low number of terms to provide the desired convergence and accuracy level. The relatively fast convergence of the series in the functions for velocity and temperature distributions makes the computer solution time efficient.

The Nusselt numbers calculated for the eight thermal versions are given in Tables 3–10 as a function of aspect ratio γ and Knudsen number Kn. The Nusselt numbers for the 4 version in Table 3 agree with the results of both Tunc and Bayazitoglu (2002) and Yu and Ameel (2002) who solved slip-flow in microchannel for the same thermal

Table 3
Nusselt numbers for the 4 version

Kn	$\gamma=0.2$	$\gamma=0.4$	$\gamma=0.6$	$\gamma=0.8$	$\gamma=1$
	Nu	Nu	Nu	Nu	Nu
0.00	2.9249	2.9906	3.0522	3.0844	3.0930
0.02	2.8962	2.9180	2.9444	2.9546	2.9501
0.04	2.7745	2.7755	2.7840	2.7834	2.7740
0.06	2.6156	2.6077	2.6074	2.6019	2.5912
0.08	2.4481	2.4370	2.4326	2.4254	2.4148
0.10	2.2857	2.2741	2.2682	2.2606	2.2509

Table 4
Nusselt numbers for the 3L version

Kn	$\gamma=0.2$	$\gamma=0.4$	$\gamma=0.6$	$\gamma=0.8$	$\gamma=1$
	Nu	Nu	Nu	Nu	Nu
0.00	3.2710	3.1799	3.1040	3.0241	2.9449
0.02	3.1410	3.0227	2.9310	2.8470	2.7699
0.04	2.9419	2.8239	2.7337	2.6547	2.5847
0.06	2.7282	2.6206	2.5381	2.4673	2.4056
0.08	2.5232	2.4285	2.3553	2.2931	2.2397
0.10	2.3353	2.2531	2.1890	2.1348	2.0884

Table 5
Nusselt numbers for the 3S version

Kn	$\gamma=0.2$	$\gamma=0.4$	$\gamma=0.6$	$\gamma=0.8$	$\gamma=1$
	Nu	Nu	Nu	Nu	Nu
0.00	2.3572	2.5613	2.7286	2.8543	2.9449
0.02	2.2923	2.4623	2.5972	2.6975	2.7699
0.04	2.1889	2.3329	2.4438	2.5256	2.5847
0.06	2.0724	2.1958	2.2886	2.3565	2.4056
0.08	1.9553	2.0620	2.1407	2.1979	2.2397
0.10	1.8433	1.9363	2.0039	2.0527	2.0884

Table 6
Nusselt numbers for the 2L version

Kn	$\gamma=0.2$	$\gamma=0.4$	$\gamma=0.6$	$\gamma=0.8$	$\gamma=1$
	Nu	Nu	Nu	Nu	Nu
0.00	5.7955	5.2916	4.8447	4.4407	4.0878
0.02	5.1443	4.6881	4.3037	3.9682	3.6778
0.04	4.4977	4.1274	3.8160	3.5453	3.3101
0.06	3.9420	3.6492	3.4002	3.1824	2.9916
0.08	3.4833	3.2514	3.0514	2.8750	2.7188
0.10	3.1072	2.9216	2.7593	2.6146	2.4855

Table 7
Nusselt numbers for the 2S version

Kn	$\gamma = 0.2$	$\gamma = 0.4$	$\gamma = 0.6$	$\gamma = 0.8$	$\gamma = 1$
	Nu	Nu	Nu	Nu	Nu
0.00	1.6640	2.5901	3.2334	3.7163	4.0878
0.02	1.6093	2.4451	2.9914	3.3842	3.6778
0.04	1.5445	2.2911	2.7552	3.0765	3.3101
0.06	1.4773	2.1422	2.5367	2.8018	2.9916
0.08	1.4118	2.0044	2.3422	2.5636	2.7188
0.10	1.3487	1.8781	2.1695	2.3563	2.4855

Table 8
Nusselt numbers for the 2C version

Kn	$\gamma = 0.2$	$\gamma = 0.4$	$\gamma = 0.6$	$\gamma = 0.8$	$\gamma = 1$
	Nu	Nu	Nu	Nu	Nu
0.00	2.3775	2.3990	2.4185	2.4286	2.4312
0.02	2.2635	2.2701	2.2781	2.2811	2.2801
0.04	2.1331	2.1334	2.1359	2.1357	2.1332
0.06	2.0032	2.0009	2.0008	1.9992	1.9962
0.08	1.8807	1.8774	1.8761	1.8740	1.8710
0.10	1.7678	1.7643	1.7625	1.7602	1.7574

Table 9
Nusselt numbers for the 1L version

Kn	$\gamma = 0.2$	$\gamma = 0.4$	$\gamma = 0.6$	$\gamma = 0.8$	$\gamma = 1$
	Nu	Nu	Nu	Nu	Nu
0.00	4.2351	3.7132	3.3003	2.9641	2.6877
0.02	3.7533	3.3238	2.9819	2.7017	2.4683
0.04	3.3350	2.9869	2.7053	2.4715	2.2748
0.06	2.9853	2.7019	2.4684	2.2720	2.1047
0.08	2.6946	2.4611	2.2657	2.0991	1.9447
0.10	2.4514	2.2567	2.0914	1.9488	1.8247

Table 10
Nusselt numbers for the 1S version

Kn	$\gamma = 0.2$	$\gamma = 0.4$	$\gamma = 0.6$	$\gamma = 0.8$	$\gamma = 1$
	Nu	Nu	Nu	Nu	Nu
0.00	0.9527	1.5871	2.0507	2.4066	2.6877
0.02	0.9264	1.5128	1.9246	2.2313	2.4683
0.04	0.8994	1.4405	1.8069	2.0737	2.2748
0.06	0.8731	1.3729	1.7003	1.9323	2.1047
0.08	0.8470	1.3090	1.6026	1.8061	1.9447
0.10	0.8219	1.2497	1.5141	1.6944	1.8247

version for developed and developing flow, respectively. The Nusselt numbers for no-slip-flow in macrochannels for all the eight thermal versions are determined by setting $Kn = 0$. The first lines on the Tables 3–10 correspond to this case. The Nusselt numbers found for no-slip-flow are in exact agreement with those of Spiga and Morini (1996) who have solved the same problem as in this paper but for macrochannels. Note that the Nusselt numbers found for the 3L and 3S, 2L and 2S, 1L and 1S, versions are equal at $\gamma = 1$, which is an expected situation. The numerical results also show that at $Kn = 0.10$ (the upper limit for slip-flow), for a given aspect ratio, the heat transfer in the 2L version is higher that that for all other thermal versions. The highest heat transfer is achieved in the 2L version with the smallest aspect ratio. For each of the thermal versions, a Nusselt number correlation in terms of aspect ratio and Knudsen number can be given by making use of the numerical values on Tables 3–10 for the purpose of practical usages.

The data on Tables 3–10 show that the Nusselt number for a microchannel with any aspect ratio decreases as the Knudsen number increases, for all the thermal versions. This means that rarefaction influences the heat transfer in the negative direction. The higher the rarefaction, the lower the heat transfer. From a geometrical point of view, this simply means that as the characteristic size of a microchannel decreases the heat transfer also decreases.

Heat transfer for the eight thermal versions may increase, decrease, or remain unchanged with aspect ratio. This is seen if the numerical values are given in graphical form. Figs. 2 and 3 show the variation of Nusselt number with aspect ratio for the 1L and 1S versions, respectively. It is seen that the heat transfer decreases for 1L version and increases for 1S version with increasing aspect ratio, which is reasonable and expected from a physical point of view. The rates of decrease for the 1L version and increase for the 1S version with increasing aspect ratio are such that they reach the same heat transfer rate at the upper limit of aspect ratio namely $\gamma = 1$, which is also expected since the 1L and 1S versions become identical versions at $\gamma = 1$. All of the observed trends given for the 1L–1S couple hold, qualitatively, for the couples 2L–2S and 3L–3S, too. The nature of the variation of heat transfer with aspect ratio for the 4 and 2C versions is completely different from the above mentioned couples. The heat transfer shows very little change with aspect ratio for these versions, as seen in Tables 3 and 8. It can be concluded that aspect ratio does

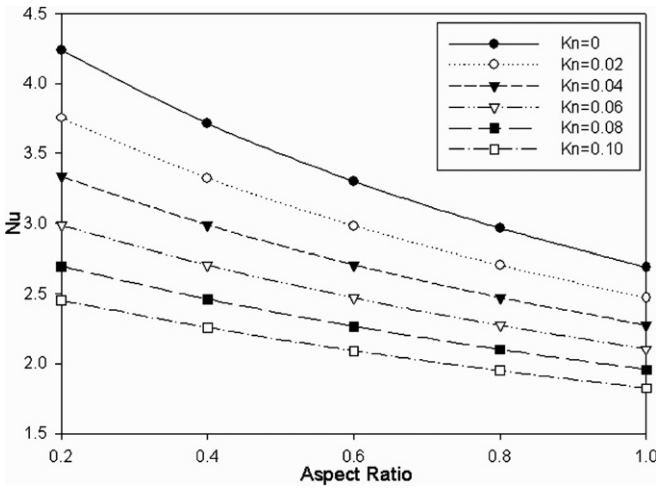

Fig. 2. Variation of Nusselt number with aspect ratio for the 1L version ($Pr = 0.6$, $R = 1.4$, $F_v = 1$, $F_t = 1$).

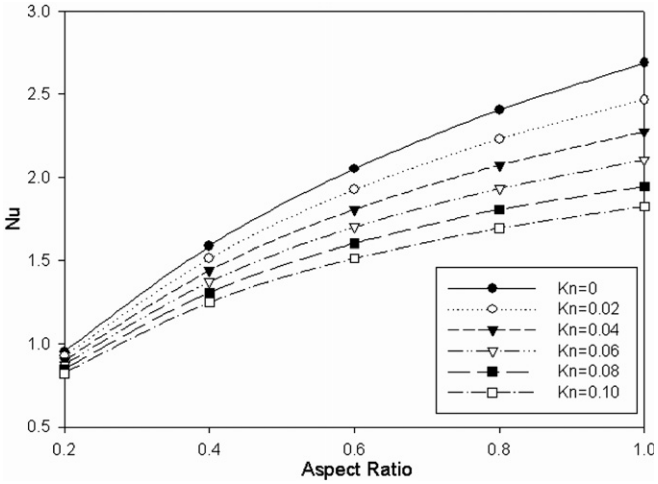

Fig. 3. Variation of Nusselt number with aspect ratio for the 1S version ($Pr = 0.6$, $R = 1.4$, $F_v = 1$, $F_t = 1$).

not affect the heat transfer strongly for 4 and 2C versions, however, for 1L, 2L and 3L versions lower aspect ratios, and for 1S, 2S and 3S versions higher aspect ratios, enhance the heat transfer.

The temperature contours for the 3L and 2C thermal versions are given in Figs. 4 and 5, respectively. The graphs

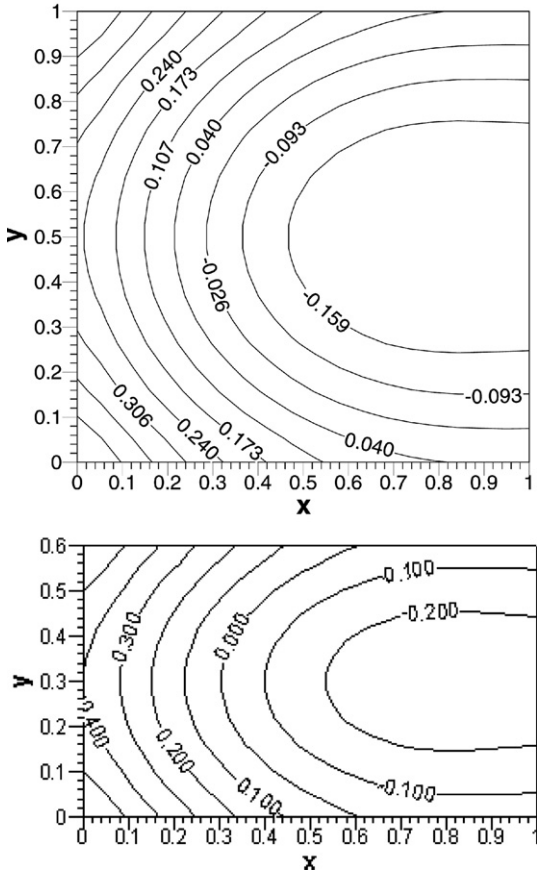

Fig. 4. Temperature contours for the 3L thermal version for $\gamma = 1$ and $\gamma = 0.6$ ($Pr = 0.6$, $R = 1.4$, $F_v = 1$, $F_t = 1$).

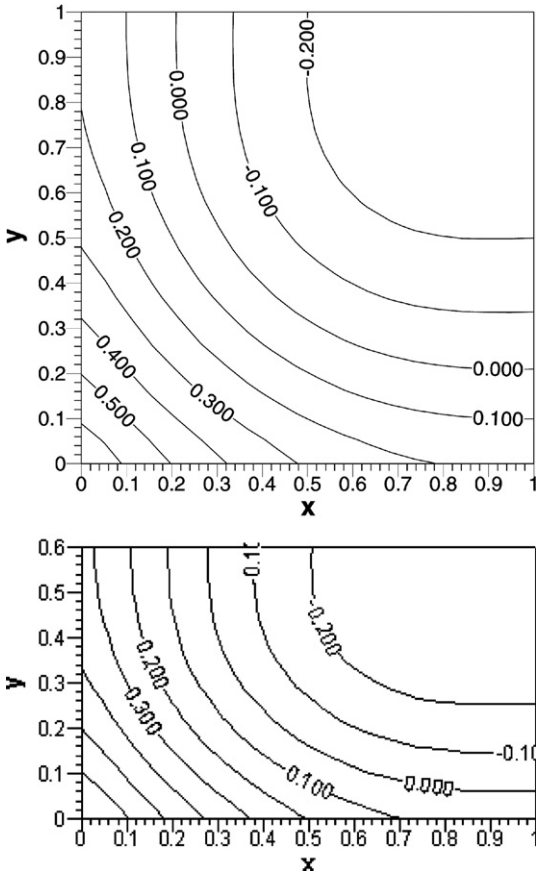

Fig. 5. Temperature contours for the 2C thermal version for $\gamma = 1$ and $\gamma = 0.6$ ($Pr = 0.6$, $R = 1.4$, $F_v = 1$, $F_t = 1$).

show constant $\hat{T}$ and not $\hat{T} + C$ lines. That is, a constant value has been dropped from the temperature values given on the graphs. This obviously would not affect the mathematical calculations if a thermal optimization of the microchannel is required. The temperature contours for each thermal version are plotted for aspect ratios equal to 0.6 and 1 at $Kn = 0.10$. Note that the temperature contours plotted in microchannels with aspect ratio equal to 1 for the, 3L and 3S, 2L and 2S and 1L and 1S versions are identical with ninety degrees geometrical rotation, as expected. The figures show that the hottest and coldest contour lines are located closest and farthest to the heated walls, respectively, which is supportive of the accuracy of the solution. Finally, it is notable that the numerical data of Tables 3–10 and the temperature contours may be used to determine the optimal geometrical and operational conditions for a microchannel exposed to any of the eight thermal versions.

9. Conclusion

The thermal behavior of a hydrodynamically and thermally developed flow in rectangular microchannels has been analyzed. The continuum approach with the velocity slip and temperature jump condition at the solid walls is applied to develop a mathematical model of the flow

phenomenon in the rectangular microchannel. A total of eight different thermal boundary conditions that are formed of different combinations of heated and adiabatic walls is considered. The solution of the mathematical model employs the velocity distribution available in the literature. Mathematical similarity between the heat conduction and convection problems is used to determine the temperature distribution in the microchannel. The solution of a heat conduction problem, available in literature, is adapted to the heat convection problem in the microchannel. The velocity and temperature distributions thus found are used to determine the average Nusselt number for all eight thermal versions. The solution method of the paper is validated for all versions for no-slip-flow conditions, and for a single thermal version (4 version) under slip-flow conditions. The paper explores the effects of rarefaction and aspect ratio on thermal character of flow in rectangular microchannels exposed to the eight different thermal boundary conditions. Numerical results are obtained for the fixed values of physical properties ($Pr = 0.6,\ R = 1.4$) and accommodation coefficients ($F_v = 1, F_t = 1$) that are representative of most engineering applications. The results show that the highest heat transfer is achieved in the microchannel with two heated long walls and two adiabatic short walls (2L version). The decreasing effect of rarefaction on heat transfer in microchannels, for all the thermal versions, is established. The higher the rarefaction, the lower the heat transfer. The numerical results also show that heat transfer for the eight thermal versions may increase, decrease, or remain unchanged with aspect ratio. In particular, heat transfer decreases for 1L, 2L and 3L versions, increases for 1S, 2S and 3S versions and, remains approximately unchanged for 4 and 2C versions with increasing aspect ratio. The solution of the paper may be used to determine the optimal geometrical and operational conditions for a microchannel exposed to any of the eight thermal versions.

Acknowledgements

The authors wish to express their gratitude to an anonymous reviewer for his/her valuable comments, suggestions and criticisms that improved the presentation of this paper considerably.

References

Barron, R.F., Wang, X., Ameel, T.A., Warrington, R.O., 1997. The Graetz problem extended to slip-flow. International Journal of Heat and Mass Transfer 40 (8), 1817–1823.

Beskok, A., Karniadakis, G.E., 1992. Simulation of slip-flows in complex micro-geometries. ASME DSC-Vol. 40, Micromechanical Systems. Book No. G00783, pp. 355–370.

Ghodoossi, L., Egrican, N., 2005. Prediction of heat transfer characteristics in rectangular microchannels for slip-flow regime and H1 boundary condition. International Journal of Thermal Sciences 44 (6), 513–520.

Hadjiconstantinou, N.G., 2003. Sound propagation at small scales under continuum and non-continuum transport. Journal of Fluid Mechanics 488, 399–408.

Hadjiconstantinou, N.G., Simek, O., 2002. Constant-wall-temperature Nusselt number in micro and nano-channels. Journal of Heat Transfer 124, 356–364.

Karniadakis, G.M., Beskok, A., 2002. Micro Flows: Fundamentals and Simulation. Springer.

Morini, G.L., 2000. Analytical determination of the temperature distribution and Nusselt numbers in rectangular ducts with constant axial heat flux. International Journal of Heat and Mass Transfer 43 (5), 741–755.

Ozisik, M.N., 1968. Boundary Value Problems of Heat Conduction. International Textbook Company, Scranton, Pennsylvania.

Spiga, M., Morini, G.L., 1996. Nusselt numbers in laminar flow for H2 boundary conditions. International Journal of Heat and Mass Transfer 39 (6), 1165–1174.

Tunc, G., Bayazitoglu, Y., 2002. Heat transfer in rectangular microchannels. International Journal of Heat and Mass Transfer 45 (4), 765–773.

Yu, S., Ameel, T.A., 2002. Slip-flow convection in Isoflux rectangular microchannels. Journal of Heat Transfer 124 (2), 346–355.